Journal of Physics: Conference Series **490** (2014) 012065 doi:10.1088/1742-6596/490/1/012065

Thermodynamic Properties and Phase Transitions of Flexible-Semiflexible Homopolymers: A Multi-Canonical Monte Carlo Simulation

Chahrazed Meddah[1], Sid Ahmed Sabeur[2], Amine Bouziane Hammou and Hadjira Medeghri

Faculté de Physique, Université des Sciences et de la Technologie d'Oran, USTOMB, BP 1505 El M'naouer, Oran 31000, Algerie

E-mail: [1]chahrazedmeddah@gmail.com, [2]sidsabeur@gmail.com

Abstract. We focus on the simulation of flexible and semiflexible polymer systems using the multicanonical Monte Carlo method where we study their thermodynamic properties and conformational behavior. First, we investigate transition signatures of flexible homopolymer chains where monomers interact through a standard Lennard-Jones potential. In the second time, we introduce a square well potential that produces helical structures. The idea behind the use of those different potentials is to construct a phase diagram where we can characterize the liquid, solid, crystalline and helical phases.

1. Introduction

Several studies have been dedicated to investigate the behavior of single polymers in different models[1, 2, 3, 4, 5, 6, 7, 8] using different methods of computer simulation like molecular dynamic and Monte Carlo method. In the present paper, we intend to consider the combination of two models: flexible and semiflexible polymer chains by adding a directional potential[6] to the Lennard-Jones potential. This study is carried out by means of multicanonical Monte Carlo method[9].

The model and the simulation method are described in Sec II. The results are given in Sec III and we conclude in Sec IV.

2. Model and simulation method

The model is described by an off lattice homopolymer chain that contains N identical monomers. In the first time, we consider the flexible chain(the same model used in references[1, 2, 5]), where all monomers interact pairwise via a truncated and shifted Lennard-Jones potential given by

$$U_{\mathrm{LJ}}(r) = 4\epsilon_{\mathrm{LJ}}\left[\left(\frac{\sigma_{\mathrm{LJ}}}{r}\right)^{12} - \left(\frac{\sigma_{\mathrm{LJ}}}{r}\right)^{6}\right] - U_{\mathrm{LJ}}\left(r_c\right) \tag{1}$$

ϵ_{LJ} is the energy scale, r denotes the relative distance between two monomers, $r_c = 2.5\sigma_{LJ}$ is the cutoff distance, and $\sigma_{LJ} = r_0 2^{\frac{-1}{6}}$ is the distance by which the potential is zero with the

minimum potential distance $r_0 = 0.7$. The interaction between nearest neighbors is given by the finite extensible nonlinear elastic FENE potential

$$U_{\mathrm{FENE}}(r) = -\frac{k}{2}R^2 \ln\left\{1 - \left[\frac{r - r_0}{R}\right]^2\right\} \tag{2}$$

k is the spring constant set to 40 and $R = 0.3$.
In the case of a flexible polymer chain, the total energy is given by

$$E_{\mathrm{tot}}^{\mathrm{flexible}} = \sum_{i=1}^{N}\sum_{j=i+1}^{N} U_{\mathrm{LJ}}(r_{ij}) + \sum_{i=1}^{N-1} U_{\mathrm{FENE}}(r_{ii+1}) \tag{3}$$

In the second time, we add a directional potential[6, 11] to study helix formation in wormlike polymer chain[12]. The interaction between monomers labeled i and j $(i, j = 1, \ldots N, i \neq j)$ is given by

$$U_{ij}^{\mathrm{helix}} = \begin{cases} 0 & \text{for} \quad \sigma_{\mathrm{helix}} \leq r_{ij} \\ -\epsilon_{\mathrm{helix}}[\hat{u}_i \cdot \hat{r}_{ij}]^6 - \epsilon_{\mathrm{helix}}[\hat{u}_j \cdot \hat{r}_{ij}]^6 & \text{for} \quad d \leq r_{ij} \leq \sigma_{\mathrm{helix}} \\ \infty & \text{for} \quad 0 \leq r_{ij} \leq d \end{cases} \tag{4}$$

where $\hat{u}_i = (\vec{r}_i - \vec{r}_{i-1})(\vec{r}_{i+1} - \vec{r}_i)/sin(\theta)$, θ is the fixed bond angle and $\hat{r}_{ij} = (\vec{r}_i - \vec{r}_j)/|\vec{r}_i - \vec{r}_j|$. Here d is the excluded volume diameter and σ_{helix} is the attractive force range. This quantities are set respectively to $3/2a$, $\sqrt{45/8}a$, a is the fixed bond length set to 0.7 and $\theta = \pi/3$. $\epsilon_{\mathrm{helix}}$ denotes the energy scale. The total energy of semiflexible polymer chains producing helical structures is given by

$$E_{\mathrm{tot}}^{\mathrm{helix}} = \sum_{i=1}^{N-1}\sum_{j=i+2}^{N-2} U_{ij}^{\mathrm{helix}} \tag{5}$$

Finally, when we combine the two potential models described above, the total energy of the chain will be

$$E_{\mathrm{tot}}(\epsilon_{LJ}, \epsilon_{\mathrm{helix}}) = E_{\mathrm{tot}}^{\mathrm{helix}} + E_{\mathrm{tot}}^{\mathrm{flexible}} \tag{6}$$

Our study is different from the other previous works[6, 11] since we are combining the two potential models and are varying the energy scales $\epsilon_{\mathrm{helix}}$ and ϵ_{LJ} which allows us to characterize the different phases. A new parameter, the ratio $\epsilon_{\mathrm{helix}}/\epsilon_{\mathrm{LJ}}$ is also used to control the simulation. To visit all possible conformations in energy space we use the multicanonical Monte Carlo method[9, 10] where the Boltzmann distribution $P_{\mathrm{can}}(E) \propto g(E)\exp(-\beta E)$ is deformed artificially in a way to produce a flat histogram and perform a random walk. Thereby, the canonical probability is multiplied by a weight factors $W(E)$ which are unknown a priori and have to be determined iteratively. The multicanonical energy distribution will be

$$P_{\mathrm{muca}}(E) \propto g(E)\exp(-\beta E)W(E) \sim H(E) = \text{constant} \tag{7}$$

$g(E)$ is the density of states and β is the inverse temperature, $\beta = 1/k_B T$. k_B is the Boltzmann constant. The iterative procedure starts by setting the weight factors $W^0(E)$ for all energies to unity and continued until the multicanonical histogram $H(E)$ is flat. In the first run, we perform a simulation at infinite temperature under canonical distribution. Each simulation n, $(n = 0, 1, 2, \ldots)$ which is performed with the estimate weights $W^n(E)$ yielding an estimate histogram $H^n(E)$. The estimation $W^{n+1}(E)$ is given by $W^{n+1}(E) = \frac{W^n(E)}{H^n(E)}$. After having estimated the appropriate weights $W(E)$, a long production run is performed to determine different statistical quantities which can be obtained by the following equation

$$\langle A\rangle_T = \frac{\sum_E A_E W^{-1}(E) e^{-\beta E}}{\sum_E W^{-1}(E) e^{-\beta E}} \tag{8}$$

The specific heat and structural quantities such as the square radius of gyration, the local and global helical order parameters H_2 and H_4 are calculated to characterize transition signatures and to specify the polymer structures.

$$R_g^2 = \frac{1}{N}\sum_{i=1}^{N}(\vec{r}_i - \vec{r}_{cm})^2 \tag{9}$$

where $\vec{r}_{cm}$ is the center of mass vector.

$$H_2 = \frac{1}{N-3}\sum_{i=2}^{N-1}\hat{u}_i \cdot \hat{u}_{i+1} \tag{10}$$

$$H_4 = \left(\frac{1}{N-2}\sum_{i=2}^{N-1}\hat{u}_i\right)^2 \tag{11}$$

3. Simulation results

In the following, we present the results of the multicanonical study in the temperature range $T \in [0, 5]$. 300 iterations are performed with 10^6 updates at each iteration to estimate the weight factors and 10^8 updates in the production run for polymer chain length of $N = 19$ monomers. The results presented below are obtained by averaging 10 simulations starting with different random seeds. The error bars of the energetic and structural quantities and their fluctuations turn out to be smaller than the data symbols used in the plots.

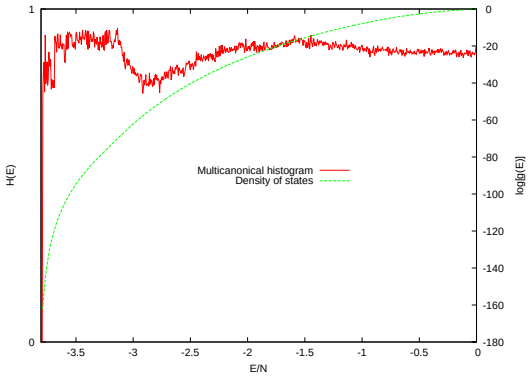

Figure 1. The multicanonical histogram and logarithm of the density of states versus energy per monomer obtained for polymer chain with N=19 and $\epsilon_{\rm LJ} \gg \epsilon_{\rm helix}$.

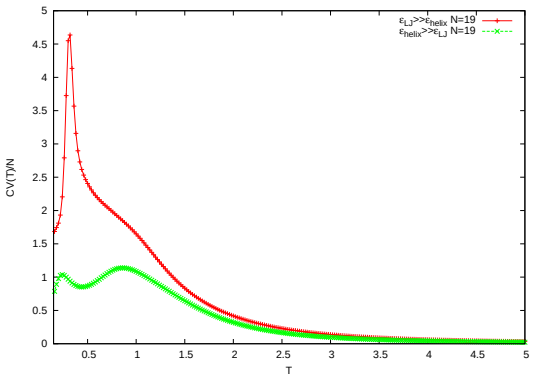

Figure 2. Specific heat versus temperature for chain length $N = 19$ in both cases $\epsilon_{\rm LJ} \gg \epsilon_{\rm helix}$ and $\epsilon_{\rm helix} \gg \epsilon_{\rm LJ}$.

In figure 1, we plot the histogram of the visited energies and the logarithm of the density of states when $\epsilon_{\rm LJ} \gg \epsilon_{\rm helix}$. Various types of displacement are used to generate conformations during the simulation. The pivot move[13] is used when $\epsilon_{\rm helix} \gg \epsilon_{\rm LJ}$, and in the other case addition to the pivot move, shift monomer, reptation, crankshaft and end-bridging moves[14] are all combined. The curves of specific heat in the two cases are plotted in figure 2. The transition is

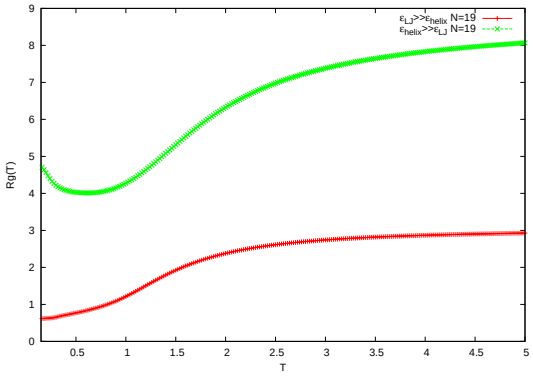

Figure 3. Radius of gyration of the chain of 19 monomers for $\epsilon_{\text{helix}} \gg \epsilon_{\text{LJ}}$ and $\epsilon_{\text{LJ}} \gg \epsilon_{\text{helix}}$.

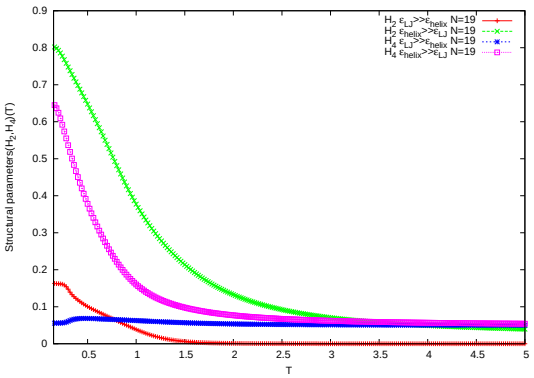

Figure 4. Structural parameters H_2 and H_4 versus temperature for chain length $N = 19$.

observed when $\epsilon_{\text{LJ}} \gg \epsilon_{\text{helix}}$ at T ≈ 0.2 and at T ≈ 0.8 for $\epsilon_{\text{helix}} \gg \epsilon_{\text{LJ}}$. Structural parameters are shown in figure 3 and 4. Snapshot of conformations obtained during the simulation representing different states are given in figure 5.

Figure 5. Representative configurations obtained during the simulation. (I):Random coil observed around $T \approx 5$. (II) and (III): Globular chains obtained for $T \approx 0.6$ and $T \approx 0.01$ when $\epsilon_{LJ} \gg \epsilon_{\text{helix}}$. (IV): Perfect helix appears for $\epsilon_{helix} \gg \epsilon_{\text{LJ}}$ at $T \approx 0.08$.

4. Conclusion

The aim of this paper is to classify flexible and semiflexible polymer chains through the study of their thermodynamic and structural properties by combining two different potential models. The preliminary results presented above are limited to two cases $\epsilon_{\text{helix}} \gg \epsilon_{\text{LJ}}$ and $\epsilon_{\text{LJ}} \gg \epsilon_{\text{helix}}$. At low temperatures, we have obtained helical conformations for the first case. The second case is dominated by the formation of globular structures. The behavior of the polymer chain at intermediate values of energy scales will be investigated in a future work where the phase diagram will be constructed.

Acknowledgments

We would like to thank Professor Michael Bachmann for helpful discussions.

References

[1] S. Schnabel, M. Bachmann and W. Janke 2009 *J. Chem. Phys.* **131** 124904
[2] S. Schnabel, W. Janke, and M. Bachmann 2011 *J. Comput. Phys.* **230** 4454
[3] S. Schnabel, T. Vogel, M. Bachmann and W. Janke 2009 *Chem. Phys. Lett* B **476** 201
[4] F. Wang and D. P. Landau 2001 *Phys. Rev. E* **64** 056101
[5] D. T. Seaton, T. Wüst and D. P. Landau 2010 *Phys. Rev. E* **81** 011802
[6] Josh P. Kemp and Zheng Yu Chen 1998 *Phys. Rev. Lett* **81** 3880

[7] M. N. Bannerman, J. E. Magee and L.Lue 2009 *Phys. Rev. E* **80** 21801
[8] Mark P. Taylor, Wolfgang Paul and Kurt Binder 2009 *Phys. Rev. E* **79** 50801
[9] B. A. Berg, T.Neuhaus 1991 *Phys. Rev. Lett. B* **267** 249
[10] B. A. Berg 1995 *J. Stat. Phys* **82**
[11] Josh P. Kemp and Jeff Z. Y. Chen 2001 *Biomacromolecules* **2** 389
[12] D. C. Rapaport 2002 *Phys Rev. E* **66** 11906
[13] N. Madras and A. D. Sokal 1988 *J. Stat. Phys* **50** 109
[14] F. A. Escobedo and J. J de Pablo 1995 *J. Chem. Phys* **102** 2636